

# Structure and Function of a Minimal Receptor Activation Domain of Parathyroid Hormone

Eun Jin Lee<sup>1</sup>, Hai-Young Kim<sup>2</sup>, Min-Kyu Cho<sup>2</sup>, Weontae Lee<sup>2</sup>, and Sung-Kil Lim<sup>1</sup>

<sup>1</sup>Department of Internal Medicine, College of Medicine, Yonsei University, Seoul, Korea;

<sup>2</sup>Department of Biochemistry, College of Science, Yonsei University, Seoul, Korea.

The structure and function of short-length amino terminal PTH analogues were studied. The substitution of Leu<sup>7</sup> with Phe in [Ala<sup>3,10</sup>Leu<sup>7</sup>Arg<sup>11</sup>]rPTH(1-11)NH<sub>2</sub> analogue peptides did not show any reduction in cAMP formation. Replacement of the 1<sup>st</sup>, 7<sup>th</sup> and 8<sup>th</sup> residues revealed different activities, depending upon the residue type. The substitution of Ala<sup>1</sup> by Ser in [Ala<sup>3,10</sup>Leu<sup>7</sup>Arg<sup>11</sup>]rPTH(1-11)NH<sub>2</sub> caused nearly a complete loss of cAMP formation. Meanwhile, NMR analysis of [(Ala<sup>1</sup>/Ser<sup>1</sup>)Ala<sup>3,10</sup>(Leu<sup>7</sup>/Phe<sup>7</sup>)Arg<sup>11</sup>]rPTH(1-11)NH<sub>2</sub> revealed an  $\alpha$ -helical backbone structure with a flexible conformation at the carboxyl-terminus. The overall results suggest that 11-residue short oligopeptide analogues of PTH tend to form an  $\alpha$ -helical structure and the different activities of those analogues could be associated with residue specificity rather than the secondary conformational structure.

**Key Words:** Parathyroid hormone, parathyroid hormone receptor, cyclic AMP-generating activity, nuclear magnetic resonance,  $\alpha$ -helix

## INTRODUCTION

Parathyroid hormone (PTH) is the major regulator of calcium and phosphate homeostasis.<sup>1</sup> Moreover, when PTH is presented in an intermittent fashion, it stimulates a net increase in bone mass.<sup>2</sup> Therefore, developing a successful

PTH analogue is viewed with considerable interest for the treatment of osteoporosis. PTH is composed of 84 amino acids, but its full biological effects are limited to its N-terminal region, PTH (1-34). However, this 34-amino acid-peptide has a low compliance problem, because the parenteral injections, nasal sprays and pulmonary inhalers are of limited effectiveness. To resolve this problem, large, in-depth studies have been conducted on the structures and functions of PTH and the PTH/PTH-related peptide (PTHrp) receptor using methods like mutagenesis analysis, cross-linking analysis, nuclear magnetic resonance (NMR) study, crystallographic analysis or homology modeling.<sup>3</sup>

Jin et al. has recently reported that hPTH(1-34) crystallizes as a slightly bent, long helical dimer.<sup>4</sup> Recent NMR analysis of hPTH(1-34) has revealed that it forms an N-terminal helix and a C-terminal helix connected by a highly flexible region in physiologic solution.<sup>5</sup> According to the report of Jin et al., the N-terminal region of PTH(1-34) binds to a pocket consisting of the extra cellular portion of TM3, TM4, TM6 and the second and third extra cellular loops of the PTH/PTHrp receptor.<sup>6</sup> The middle region of PTH(1-34) is sandwiched between the first extra cellular loop and the N-terminal extra cellular region of the receptor adjacent to TM1, and the C-terminal region of hPTH(1-34) interacts extensively with the putative binding domain of the PTH/PTHrp receptor. After comparing their crystallographic data with published NMR data on PTH(1-34), Jin et al. proposed that only one orientation of hPTH(1-34) satisfied all the known ligand receptor interactions. Furthermore, it was recently reported that

Received March 27, 2004

Accepted May 12, 2004

This work was supported by research grants from the Korea Ministry of Health and Welfare (HMP-01-PJ1-PG1-01CH08-0001) and Brain Korea 21 Project for Medical Science.

Reprint address: requests to Dr. Sung-Kil Lim, Division of Endocrinology, Department of Internal Medicine, Yonsei University College of Medicine, 134 Shinchon-dong, Seodaemun-gu, Seoul 120-752, Korea. Tel: 82-2-361-5432, Fax: 82-2-393-6884, E-mail: lsk@yumc.yonsei.ac.kr

Tip39 is an endogenous ligand of the PTH2 receptor,<sup>7,8</sup> and that the NMR structure of Tip39 helps to explain the manner in which PTH(1-34) binds to the PTH/PTHrp receptor.<sup>9</sup>

For PTH(1-34), the amino-terminal portion is critical for PTH/PTHrp receptor activation.<sup>10,11</sup> Shimizu et al. showed that PTH(1-14)NH<sub>2</sub> weakly stimulated cAMP formation, to the ca. 1/1000 of that of hPTH(1-34) in LLC-PK cells stably expressing a high level of the hPTH/PTHrp receptor.<sup>12</sup> Furthermore, they substituted PTH residues and analyzed the functional tolerability of each residue substitutions. Finally, they proposed that the short amino-terminal peptides of PTH could possibly be optimized to significantly increase signaling potency by modifying the interactions involving receptor regions containing the transmembrane domains and the extra cellular loops.<sup>13-15</sup> However, although a part has just been explored and is being currently tested by some research groups, such shorter and more potent PTH analogues have not been fully developed to date. Furthermore, few studies have been conducted upon the structures and functions of derivatives of PTH(1-11), PTH(1-12) or PTH(1-13).<sup>12,16,17</sup>

PTH(1-14) is regarded as the basic entity required for receptor activation, but the functionality of PTH(1-14) required for PTH/PTHrp receptor activation is retained in the first 9 amino acids.<sup>15</sup> Accordingly, little work has been reported upon the relationships between the structures and functions of amino acids 9 to 14 N-terminal PTH analogues.<sup>12,16,17</sup> Moreover, in previous studies, the substitution of the 1<sup>st</sup>-6<sup>th</sup> amino acids residues was found to cause the loss of the receptor activating function.<sup>18,19</sup> To better understand the ligand and receptor interactions of the short N-terminal PTH fragment activating the PTH/PTHrp receptor, and to develop more potent analogues, we systemically synthesized 11-residue-length amino terminal PTH analogues that were substituted at the 1<sup>st</sup>, 7<sup>th</sup> and 8<sup>th</sup> amino-acids whilst preserving the 2<sup>nd</sup>-6<sup>th</sup> amino acids residues. The biological activities of these analogues were examined using a cAMP-generating assay in LLC-PK1 cell lines stably transfected with the wild-type human PTH1 receptor, and NMR was used to determine their conformational characteristics.

## MATERIALS AND METHODS

### Chemicals

All media and sera for cell cultivation were purchased from Gibco-BRL (Grand island, NY, USA). hPTH(1-34) and other chemicals mentioned were purchased from Sigma-Aldrich Korea (Saint Louis, Missouri, USA), unless specified otherwise.

### Peptide synthesis

Modified rPTH(1-11) analogues were made with substitutions at the 1<sup>st</sup>, 7<sup>th</sup> or 8<sup>th</sup> residues (Table 1). These residues are known to tolerate substitution more than the first 6 residues of the N-terminus, as described by Shimizu et al.<sup>12</sup> All synthesized peptides had an amide group at the C-terminus. The peptides used in this study were synthesized at Korea Basic Science Institute (Seoul, Korea) using the solid phase approach and they were purified by HPLC. Peptide sequences were assembled with Milligen 9050 (Fmoc Chemistry). For deprotection, reagent mixture (88% trifluoroacetic acid, 5% phenol, 2% triisopropylsilane, 5% H<sub>2</sub>O; 2 h) was used. The raw peptides were purified by HPLC (Delta PAK 15 $\mu$  C18 300Å 3.9  $\times$  150 mm column), with a 240 nm detector. Mass spectroscopy was used to confirm the molecular masses of the synthesized peptides.

### Expression of PTH receptor clones and cell culture

Human Type-1 parathyroid hormone receptor (hPTH1R) cDNA, kindly provided by the Mogam Biotech Institute (Sungnam, Korea), was cloned into the expression vector pcDNA3 neo. By using a PCR cloning technique, they were able to obtain a 1.8 Kb hPTH1R cDNA that included the total open reading frame of hPTH1R, as referenced from the human kidney library. For receptor expression, LLC-PK1 porcine kidney cells were grown in Medium-199 with 3% fetal bovine serum (FBS) in 95% O<sub>2</sub>/5% CO<sub>2</sub>, and the cells were stably transfected with hPTH1R-pcDNA3 neo using the calcium phosphate method. Briefly, 5 - 7  $\times$  10<sup>5</sup> cells (approximately 80% confluent cultures) were plated on 10 cm culture dishes the day before

transfection. The cells were nourished with fresh complete culture medium containing 20 mM Hepes and then incubated in 95% O<sub>2</sub>/5% CO<sub>2</sub>. After 3-4h, the medium was discarded and 5 ml of calcium phosphate-DNA precipitate containing 25 µg DNA, 124 mM CaCl<sub>2</sub>, 140 mM NaCl, 25 mM Hepes and 1.41 mM Na<sub>2</sub>HPO<sub>4</sub> (pH 7.12) was added. The cells were then incubated for 4h in 95% O<sub>2</sub>/5% CO<sub>2</sub>, washed with NaCl/Pi (137 mM NaCl, 2.68 mM KCL, 4.3 mM Na<sub>2</sub>HPO<sub>4</sub>, 1.47 mM KH<sub>2</sub>PO<sub>4</sub>, pH 7.12), shocked with glycerol buffer (15% glycerol, 140 mM NaCl, 25 mM Hepes and 1.41 mM Na<sub>2</sub>HPO<sub>4</sub>, pH 7.12), re-washed with NaCl/Pi, and incubated for an additional 36-48h in complete Medium-199. The cells were then cultured in complete Medium-199 containing 0.5 mg/ml G418 (Geneticin; Life Technologies) until the G418-resistant colonies appeared, and these were then picked out and subcultured for at least 10-14 days. Human PTH1R-expressing cells were identified by screening more than 30 colonies, and the cells were confirmed using the hPTH(1-34) induced cAMP accumulation assay, as described below. The LLC-PK1 porcine kidney cell with the highest reactivity (clone 4), stably transfected with human PTH1R cDNA, was selected for further study. The number of hPTH1 receptors was determined to be 800,000 receptors/cell by competitive radioligand binding assay using <sup>125</sup>I-[Nle<sup>8,18</sup>Tyr<sup>34</sup>] bPTH(1-34) and Scatchard plotting, as previously described.<sup>20</sup>

#### cAMP generating assay

LLC-PK1 cells expressing the receptors were grown to confluence in 48-well plates. Cell culture medium was changed to complete Medium-199 containing 3% FBS 3-4hrs before the cells were treated with peptides. For the assays, the medium was first removed and the cells were washed with 0.25 ml of cAMP-generating medium containing 3% FBS, 2 mM 3-isobutyl-1-methyl-xanthine, 0.1% BSA, 20 mM Hepes, and 0.002% ascorbic acid in complete Medium-199. cAMP-generating media (0.15 ml) containing various concentrations of peptides were added and the cells were incubated for 30 mins at 37°C. The media was then completely discarded, and the cells frozen at -70°C for 30 min and thawed at room temperature for 15-

20 mins; this freeze-thawing process was repeated twice. The cells were then detached from the plates with 0.5 ml of 50 mM HCl solution per well, transferred to a 1.5 ml Eppendorf tube and centrifuged at 1900 × g for 10 min. The supernatants were then diluted 50-fold with radio-immunoassay (RIA) buffer and the cAMP concentration was measured using a cAMP <sup>125</sup>I RIA Kit (Stoughton, MA, USA), according to the manufacturer's instructions. The mean values of the data were fitted to a sigmoid curve with a variable slope factor using the nonlinear squares regression technique in the GRAPHPAD PRISM. EC<sub>50</sub> (nM) values are represented by means ± SE. All of the cAMP assays were performed in triplicate wells and repeated twice. (*p* < 0.05 was considered significant).

#### Circular dichroism (CD) spectroscopy

CD spectra of the peptide samples in H<sub>2</sub>O with various concentrations of trifluoroethanol (TFE) were recorded at room temperature using a Jasco J-715 spectropolarimeter (Rheinstetten, Germany). The concentrations of the peptides ranged from 79 µM to 81 µM in 50 mM phosphate buffer at pH 7.0, and the CD spectra were recorded from 190 to 250 nm at a scanning rate of 50 nm · min<sup>-1</sup> with a time constant of 0.5 s. CD data were obtained from an average of 7 scans with a resolution of 0.2 nm and bandwidth of 2.0 nm. A standard noise reduction was applied to the final spectrum.

#### NMR spectroscopy and modeling calculations

NMR spectroscopy was carried out in both 70% H<sub>2</sub>O (D<sub>2</sub>O)/30% 2,2,2-trifluoro-(d<sub>3</sub>)-ethanol (TFE) and 90% H<sub>2</sub>O/10% D<sub>2</sub>O at pH 7.0. The peptide concentrations were 3.2 mM for [Ser<sup>1</sup>Ala<sup>3,10</sup>Leu<sup>7</sup>Arg<sup>11</sup>]rPTH(1-11)NH<sub>2</sub> and [Ala<sup>3,10</sup>Phe<sup>7</sup>Arg<sup>11</sup>]rPTH(1-11)NH<sub>2</sub> in 50 mM of sodium phosphate buffer. NMR spectra were recorded at 298K on a Bruker DRX-500 spectrometer (Rheinstetten, Germany) equipped with a triple resonance probe and triple axis gradient coils. The spectra were also recorded over the temperature range 10-25°C to calculate the temperature coefficients. Pulsed-field gradient (PFG) technique was used in all H<sub>2</sub>O experiments

to suppress solvent signals. Two-dimensional total correlation spectroscopy (TOCSY)<sup>21</sup> with an MLEV-17 mixing pulse of 69.7 ms, and two-dimensional nuclear Overhauser effect spectroscopy (NOESY)<sup>22</sup> with mixing times of 100-600 ms were also performed. Two-dimensional double-quantum-filtered (DQF) COSY<sup>23</sup> spectra were collected in H<sub>2</sub>O to obtain the vicinal coupling constants. A series of one-dimensional NMR measurements were obtained to identify the slowly exchanging amide hydrogen resonance in freshly prepared D<sub>2</sub>O solutions after the H<sub>2</sub>O sample had been lyophilized. All NMR experiments were performed in the phase-sensitive mode using the Time Proportional Phase Incrementation (TPPI) method<sup>24</sup> with 2048 data points in  $t_2$  domains, and 256 points in  $t_1$  domains. NMR data were processed using XWIN-NMR (Bruker Instruments, Rheinstetten, Germany) software, and the processed data further analyzed using Sparky 3.60 software, which was developed at UCSF on a Silicon Graphics Indigo<sup>2</sup> workstation. Starting structures were generated using distance geometry (DG) by employing a refinement protocol using distance restraints assigned as strong, medium or weak on the basis of cross-peak volumes in the NOESY spectra. All distances had a lower limit of 1.8 Å, with upper limits of 2.7, 3.3 or 5.0 Å for strong, medium or weak intensities, respectively. The dihedral angle constraints were also deduced from the  $^3J_{\text{HN}\alpha}$  coupling constants from the 2D double-quantum-filtered correlated spectroscopy (DQF-COSY) spectra in H<sub>2</sub>O. Structure calculations were performed using hybrid distance geometry and dynamical simulated-annealing protocol<sup>25-28</sup> using CNS ver. 1.1<sup>29</sup> on a Linux (Red-Hat 7.0) system.

## RESULTS AND DISCUSSION

### Effects of the synthesized peptides on cAMP accumulation in LLC-PK1 cells stably expressing human Type-1 parathyroid hormone receptor (hPTH1R)

LLC-PK1 cells stably transfected with human PTH1R cDNA were stimulated with the synthesized PTH analogues. Parental LLC-PK1 cells,

which did not express hPTH1 receptors, were unresponsive to hPTH(1-34) or any of the PTH analogues used in this study (data not shown). However human PTH1R-expressing cells were responsive to hPTH(1-34) ( $\text{EC}_{50} = 50.93 \pm 0.13$  pM) and our PTH analogues, and they showed a basal activity that was similar to that of untransfected LLC-PK1 cells without hPTH(1-34) treatment. A typical dose-dependent induction of cAMP generating activity was observed upon increasing the concentrations of the PTH analogues, and the  $\text{EC}_{50}$  values calculated from the dose-response curves proved reproducible over several experiments; the results are summarized in Table 1.

### Effect of substitution in the 1<sup>st</sup>, 7<sup>th</sup> and 8<sup>th</sup> residues

Substitution of Leu<sup>7</sup> by Phe in [Ala<sup>3,10</sup>Phe<sup>7</sup>Arg<sup>11</sup>]rPTH(1-11)NH<sub>2</sub> preserved cAMP production; however, substitution of Leu<sup>7</sup> by dPhe, Val or Ile remarkably reduced cAMP accumulation (Fig. 1A). In addition, Met<sup>8</sup>, which is vulnerable to oxidation, was substituted by Leu<sup>8</sup> or norleucine (Nle<sup>8</sup>) to confirm that oxidation is critical. Substituting Met<sup>8</sup> with Nle had little effect upon cAMP activity; however, substituting it with Leu reduced cAMP activity 10 fold (Fig. 1B), which may be due to the shorter side chain of the Leu residue. Meanwhile, when Ser was introduced as the first residue in [Ser<sup>1</sup>Ala<sup>3,10</sup>Leu<sup>7</sup>Arg<sup>11</sup>]rPTH(1-11)NH<sub>2</sub>, cAMP generating activity was almost undetectable, but the substitution of the Ala<sup>1</sup> of [Ala<sup>3,10</sup>Phe<sup>7</sup>Arg<sup>11</sup>]rPTH(1-11)NH<sub>2</sub> by Ser<sup>1</sup> restored cAMP activity (Table 1).

### Circular dichroism (CD)

In order to determine why the biological activities of the rPTH(1-11) analogues differ by substitutions, we determined the solution structures of [Ser<sup>1</sup>Ala<sup>3,10</sup>Leu<sup>7</sup>Arg<sup>11</sup>]rPTH(1-11)NH<sub>2</sub> and [Ala<sup>3,10</sup>Phe<sup>7</sup>Arg<sup>11</sup>]rPTH(1-11)NH<sub>2</sub>. First, CD spectra were acquired for the rPTH analogues under different conditions. [Ser<sup>1</sup>Ala<sup>3,10</sup>Leu<sup>7</sup>Arg<sup>11</sup>]rPTH(1-11)NH<sub>2</sub> and [Ala<sup>3,10</sup>Phe<sup>7</sup>Arg<sup>11</sup>]rPTH(1-11)NH<sub>2</sub> peptides were found to have essentially helical conformations; as is shown in Fig. 2.

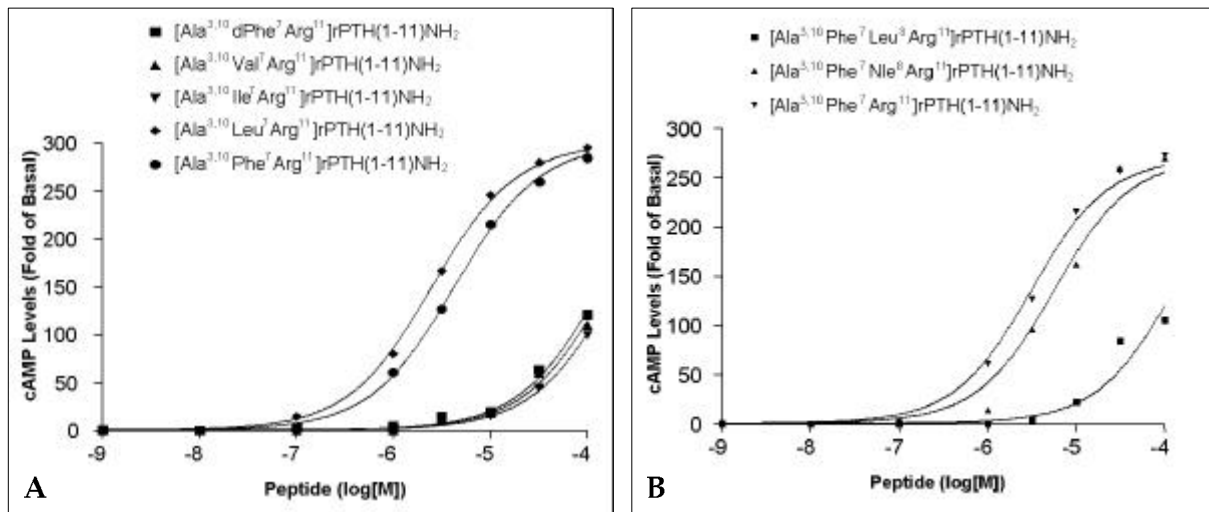


**Fig. 1.** cAMP formation of various PTH analogues in LLC-PK1 cells stably transfected with hPTH1R. (A) The effect of 7<sup>th</sup> residue substitution in  $[Ala^{3,10}Leu^7Arg^{11}]rPTH(1-11)NH_2$  with Phe, dPhe, Val, Ile, or Leu on cAMP activity. (B) The effects of 8<sup>th</sup> residue substitution Met<sup>8</sup> in the  $[Ala^{3,10}Phe^7Arg^{11}]rPTH(1-11)NH_2$  analogue with Leu, Nle or Ala. Each experiment was performed in duplicate and repeated three times. The symbols are defined in the figure key, and the curves were fitted to the data points by non-linear regression analysis, as described in Materials and Methods. The amino acid sequence of native rPTH(1-11) is AVSEIQLMHNL.

**Table 1.** EC<sub>50</sub> Values (means  $\pm$  SEM) of the rPTH(1-11) Analogues Used in This Study

Analogue (7 <sup>th</sup> modification) sequence	EC <sub>50</sub> (nM)	Analogue (Phe <sup>7</sup> ) sequence	EC <sub>50</sub> (nM)
$[Ala^{3,10}Phe^7Arg^{11}]rPTH(1-11)NH_2$	1529 $\pm$ 81.695	$[Ala^{3,10}Phe^7Arg^{11}]rPTH(1-11)NH_2$	2132 $\pm$ 126.24
$[Ser^1Ala^{3,10}Leu^7Arg^{11}]rPTH(1-11)NH_2$	—	$[Ser^1Ala^{3,10}Leu^7Arg^{11}]rPTH(1-11)NH_2$	4230 $\pm$ 136.26
$[Ala^{3,10}dPhe^7Arg^{11}]rPTH(1-11)NH_2$	—	$[Ala^{3,10}Phe^7Asp^{10}Arg^{11}]rPTH(1-11)NH_2$	—
$[Ala^{3,10}Val^7Arg^{11}]rPTH(1-11)NH_2$	—	$[Ala^{3,10}Phe^7Gln^{10}Arg^{11}]rPTH(1-11)NH_2$	—
$[Ala^{3,10}Ile^7Arg^{11}]rPTH(1-11)NH_2$	—	$[Ala^{3,10}Phe^7Leu^8Arg^{11}]rPTH(1-11)NH_2$	—
		$[Ala^{3,10}Phe^7Nle^8Arg^{11}]rPTH(1-11)NH_2$	3256 $\pm$ 752.62

All peptides have an amide group at the C-terminus. The main substituted amino-acid residues are shown in bold italics. — : mature cAMP generation failed to reach the maximum levels achieved by other ligands.

The amino acid sequence of native rPTH(1-11) is AVSEIQLMHNL. EC<sub>50</sub> values were obtained by computer analysis of the respective dose-response curves on hPTH1R stably transfected LLC-PK1 cell lines. Data are represented as means  $\pm$  SE of least three independent experiments.

CD spectra in aqueous solutions were measured at a peptide concentration of 20  $\mu$ M under benign conditions, i.e., in 50 mM sodium phosphate, pH 7.0, at 25°C. Fig. 2 shows that the helix populations of both peptides were very low in 100% aqueous solution, but in the TFE environment both peptides possess a degree of helical structure, based on the ellipticity at 222 nm, and the characteristic  $\alpha$ -helical transition, a typical double minimum ( $n-\pi^*$  transition) at 208 and 222 nm, and a maximum ( $\pi-\pi^*$  transition) at 192 nm. In SDS solution, the CD spectra indicated the presence of

typical helix conformations (data not shown). In the case of peptides in 50% (v/v) TFE/H<sub>2</sub>O solution at 25°C, pH 7.0, the CD spectrum showed a clear double minimum at 208 and 222 nm, thus indicating the presence of a significant  $\alpha$ -helix population, but the proportions were different.  $[Ser^1Ala^{3,10}Leu^7Arg^{11}]rPTH(1-11)NH_2$  shows less of a helical population than  $[Ala^{3,10}Phe^7Arg^{11}]rPTH(1-11)NH_2$ , which was derived from a helix-proportion calculation by an embedded CD analysis program (data not shown). This decreased helical conformation of  $[Ser^1Ala^{3,10}Leu^7Arg^{11}]rPTH$

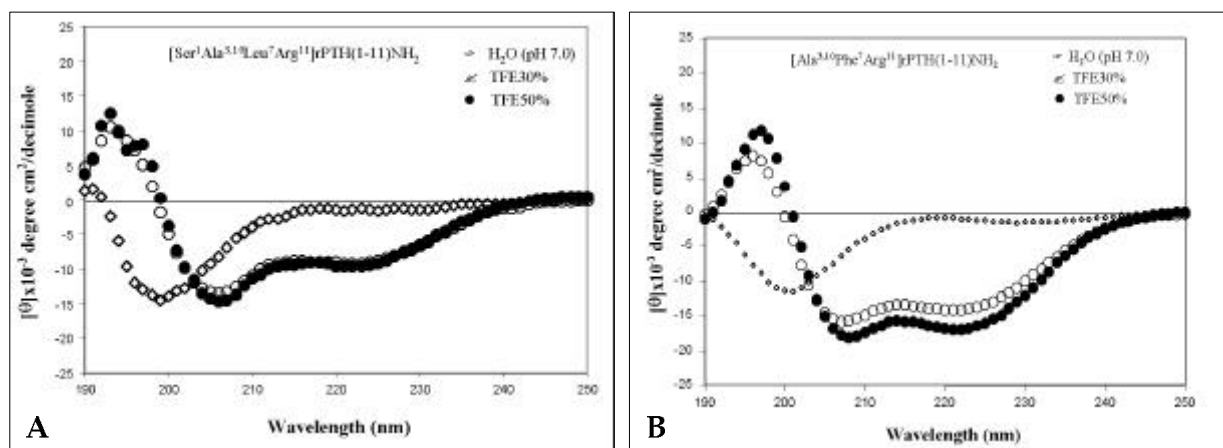


**Fig. 2.** Circular dichroism spectra of (A) [Ser<sup>1</sup>Ala<sup>3,10</sup>Leu<sup>7</sup>Arg<sup>11</sup>]rPTH(1-11)NH<sub>2</sub>, (B) [Ala<sup>3,10</sup>Phe<sup>7</sup>Arg<sup>11</sup>]rPTH(1-11)NH<sub>2</sub> in different solutions; H<sub>2</sub>O (◇), 30% TFE (■), 50% TFE (●) at pH 7.0 and 298K.

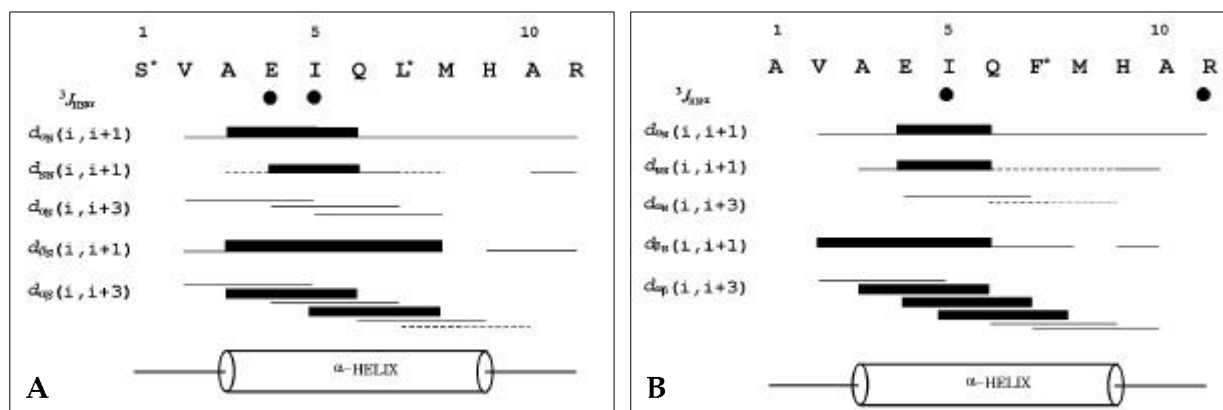


**Fig. 3.** Summary of the NMR data of (A) [Ser<sup>1</sup>Ala<sup>3,10</sup>Leu<sup>7</sup>Arg<sup>11</sup>]rPTH(1-11)NH<sub>2</sub>, and (B) [Ala<sup>3,10</sup>Phe<sup>7</sup>Arg<sup>11</sup>]rPTH(1-11)NH<sub>2</sub> in an aqueous 30% TFE solution at pH 7.0 and 298K, showing sequential and short-range NOE contacts. The strength of the observed NOEs is represented by the line thickness. The dashed line represents NOEs unresolved by resonance overlapping. Vicinal coupling constants (●; 3JHN(<6 Hz) are indicated and the helical region is represented by a cylinder.

(1-11)NH<sub>2</sub> was thought to come from the hydrophilic Ser<sup>1</sup> residue, which makes [Ser<sup>1</sup>Ala<sup>3,10</sup>Leu<sup>7</sup>Arg<sup>11</sup>]rPTH(1-11)NH<sub>2</sub> unable to have any effect on PTHR.

### Resonance assignment and solution structure

To determine the differences of both peptides, the solution structures of both peptides were determined. Complete proton resonance assignments were possible using the standard sequential resonance assignment procedure.<sup>30</sup> Having classified the individual spin systems, backbone sequential resonances were assigned using  $d_{\alpha N}(i, i+1)$  NOE connectivities in the 2D-nuclear Over-

hauser effect spectroscopy (NOESY) spectra. A number of well-resolved, intense  $d_{NN}$  cross-peaks were also observed, suggesting the formation of an  $\alpha$ -helix. Fig. 4 summarizes the sequential and short-range NOE connectivities observed for the rPTH analogues in 30% TFE. The observation of continuous  $d_{NN}(i, i+1)$  contacts, together with the characteristic  $d_{\alpha N}(i, i+3)$  and the  $d_{\alpha\beta}(i, i+3)$  NOEs, supports the existence of  $\alpha$ -helices containing Ala<sup>3</sup>-His<sup>9</sup> residues in both rPTH analogues (Fig. 3).

The NMR structures were calculated using the experimental restraints derived from 2D-NOESY and double-quantum-filtered correlated spectroscopy (DQF-COSY) spectra. A total of 50 distance

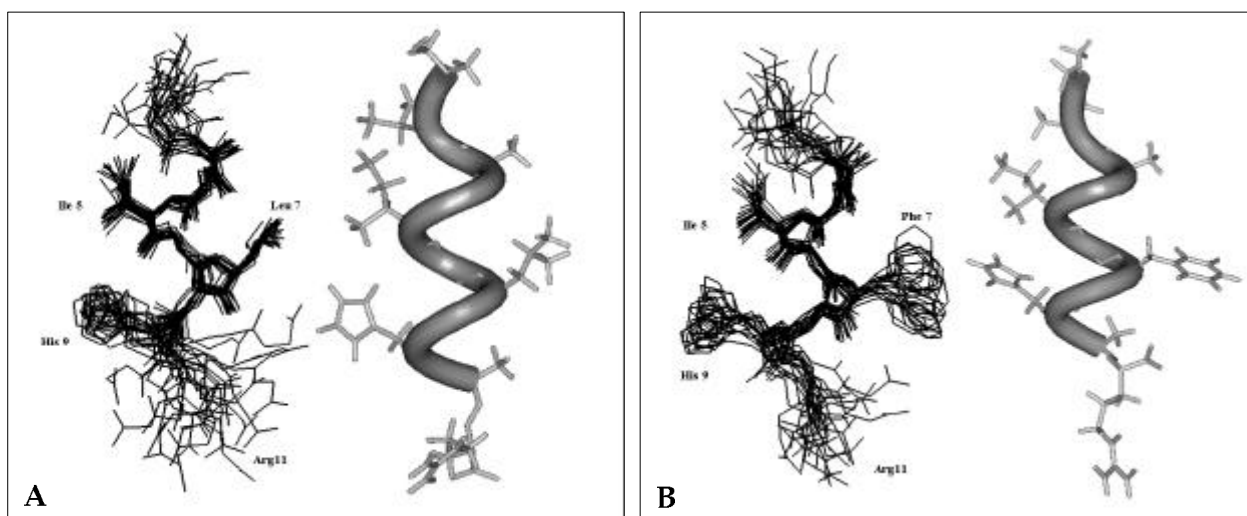


**Fig. 4.** NMR structures of the rPTH(1-11)NH<sub>2</sub> analogues. Superposition of the final 20  $\langle SA \rangle_k$  structures upon the energy-minimized average structure ( $\langle SA \rangle_{kr}$ ) of Ala<sup>3</sup>-His<sup>9</sup>, and ribbon drawings of the REM structures of (A) [Ser<sup>1</sup>Ala<sup>3,10</sup>Leu<sup>7</sup>Arg<sup>11</sup>]rPTH(1-11)NH<sub>2</sub>, and (B) [Ala<sup>3,10</sup>Phe<sup>7</sup>Arg<sup>11</sup>]rPTH(1-11)NH<sub>2</sub> in an aqueous 30% TFE solution at pH 7.0 and 298K.

**Table 2.** Structural Statistics for the 20 Final Simulated-annealing Structures

	[Ser <sup>1</sup> Ala <sup>3,10</sup> Leu <sup>7</sup> Arg <sup>11</sup> ] rPTH(1-11)NH <sub>2</sub>		[Ala <sup>3,10</sup> Phe <sup>7</sup> Arg <sup>11</sup> ] rPTH(1-11)NH <sub>2</sub>	
	$\langle SA \rangle_k$	$\langle SA \rangle_{kr}$	$\langle SA \rangle_k$	$\langle SA \rangle_{kr}$
(A) RMSD from experimental distance restraints (Å)				
all	0.0129	0.0118	0.0084	0.0131
sequential ( $ i-j =1$ )	0.0192	0.0189	0.0135	0.0218
intraresidue	0.002	0	0	0
interresidue	0.0152	0.0149	0.0109	0.0169
(B) RMSD from experimental dihedral restraints (deg)				
dihedral angle restraints	0.4566	0.4457	0.4346	0.436
(C) Energies (kcal/mol)				
$E_{total}$	11.41	12.42	9.794	10.29
$E_{NOE}$	0.7968	0.5532	0.2705	0.0067
$E_{tor}$	10.26	9.774	9.264	9.321
$E_{repel}$	0.3941	0.0008	0.0142	0.0067
$E_{L-J}^a$	-135.7	-126.7	-146.4	-145.4
(D) Deviation from idealized covalent geometry				
bond (Å)	0.0011	0.0005	0.0009	0.0011
angles (deg)	0.4566	0.4457	0.4346	0.436
impropers(deg)	0.091	0.0812	0.086	0.0894

<sup>a</sup> $E_{L-J}$  is the Lennard-Jones/van der Waals potential calculated using CHARMM empirical energy functions.

geometry (DG) structures served as the starting structures for the dynamic simulated-annealing (SA) calculations of the peptides in TFE solutions. The 20 lowest energy structures ( $\langle SA \rangle_k$ ) from the

50 simulated-annealing structures were selected for detailed structural analysis (Table 2). The average structure ( $\langle SA \rangle_k$ ) was calculated from the geometrical average of the 20  $\langle SA \rangle_k$  structural

coordinates, and restraint energy minimization (REM) was used to correct covalent bonds and angular distortions. In Fig. 4, the final 20 structures are displayed as superimposed structures ( $\langle SA \rangle_k$ ) of rPTH(1-11). A Ramachandran plot (data not shown) for all 20  $\langle SA \rangle_k$  structures showed that the  $\phi$ , and  $\psi$  angles of the final simulated-annealing structures are distributed adequately in energetically acceptable regions. The main secondary structural feature of the rPTH analogues is the  $\alpha$ -helix spanning residues of Ala<sup>3</sup>-His<sup>9</sup> in 30% TFE/H<sub>2</sub>O solution. Although both the peptides show helical conformations, their stabilities are different when considering the Lennard-Jones/ van der Waals potential energy in Table 2.

In this study, we show that short oligopeptides, based on the first 11 amino acids of PTH, tend to form an  $\alpha$ -helical structure, and that the activity differences observed for the short amino terminal analogues might be explained by residue specificity in terms of optimum receptor pocket binding and helix stability. We hope that the results of this study will assist in the understanding of the structure-activity relationships of short amino terminal oligopeptides, and this will provide a future direction for the development of low molecular weight PTH analogues.

## ACKNOWLEDGMENTS

We thank the Mogam Biotech. Institute (Sungnam, Korea) for providing the human PTH1R cDNA.

## REFERENCES

1. Potts JT Jr, Bringham FR, Gardella T, Nussbaum S, Serge G, Kronenberg H. Williams' Textbook of Endocrinology. In: Williams RH, Wilson JD, Forster DW, editors. Philadelphia: W.B. Saunders Co.; 1995. p.920-66.
2. Rodan GA, Martin TJ. Therapeutic approaches to bone diseases. *Science* 2000;289:1508-14.
3. Bisello A, Adams AE, Mierke DF, Pellegrini M, Rosenblatt M, Suva LJ, et al. Parathyroid hormone-receptor interactions identified directly by photocross-linking and molecular modeling studies. *J Biol Chem* 1998;273:22498-505.
4. Jin L, Briggs SL, Chandrasekhar S, Chirgadze NY, Clawson DK, Schevitz RW, et al. Crystal Structure of human parathyroid hormone 1-34 at 0.9-Å resolution. *J Biol Chem* 2000;275:27238-44.
5. Pellegrini M, Royo M, Rosenblatt M, Chorev M, Mierke DF. Addressing the tertiary structure of human parathyroid hormone-(1-34). *J Biol Chem* 1998;273:10420-7.
6. Mannstadt M, Juppner H, Gardella TJ. Receptors for PTH and PTHrP: their biological importance and functional properties. *Am Physiol Soc (Invited Review)*. 1999. p.F665-75.
7. Hoare SR Jr, Clark JA, Usdin TB. Molecular determinants of tuberoinfundibular peptide of 39 residue (TIP39) selectivity for the parathyroid hormone-2 (PTH2) receptor (N-terminal truncation of TIP39 reverses PTH2 receptor/PTH1 receptor binding selectivity). *J Biol Chem* 2000;275:27274-83.
8. Usdin TB, Wang T, Hoare SR Jr, Mezey E, Palkovits M. New members of the parathyroid hormone/parathyroid hormone receptor family: The parathyroid hormone 2 receptor and tuberoinfundibular peptide of 39 residues. *Front Neuroendocrinol* 2000;21:349-83.
9. Piserchio A, Usdin TB, Mierke DF. Structure of Tuberoinfundibular peptide of 39 residues. *J Biol Chem* 2000;275:27284-90.
10. Takasu H, Gardella TJ, Luck MD, Potts JT Jr, Bringham FR. Amino-terminal modifications of human parathyroid hormone (PTH) selectively alter phospholipase C signaling via the type 1 PTH receptor: Implications for design of signal-specific PTH ligands. *Biochemistry* 1999;38:13453-60.
11. Juppner H, Schipani E, Bringham FR, McClure I, Keutmann HT, Potts JT Jr, et al. The extracellular amino-terminal region of the parathyroid hormone (PTH)/PTH-related peptide receptor determines the binding affinity for carboxyl-terminal fragments of PTH (1-34). *Endocrinology* 1994;134:879-84.
12. Shimizu M, Potts JT Jr, Gardella TJ. Minimization of parathyroid hormone (Novel amino-terminal parathyroid hormone fragments with enhanced potent in activating the type-1 parathyroid hormone receptor). *J Biol Chem* 2000;275:21836-43.
13. Piserchio A, Bisello A, Rosenblatt M, Chorev M, Mierke DF. Characterization of parathyroid hormone/receptor interactions: Structure of the first extracellular loop. *Biochemistry* 2000;39:8153-60.
14. Pellegrini M, Bisello A, Chorev M, Mierke DF. Binding domain of human parathyroid hormone receptor: From conformation to function. *Biochemistry* 1998;37:12737-43.
15. Luck MD, Carter PH, Gardella TJ. The (1-14) fragment of parathyroid hormone (PTH) activates intact and amino-terminally truncated PTH-1 receptors. *Mol Endocrinol* 1999;13:670-80.
16. Shimizu N, Guo J, Gardella TJ. Parathyroid hormone (PTH)-(1-14) and -(1-11) analogs conformationally constrained by  $\alpha$ -aminoisobutyric acid mediate full agonist responses via the juxtamembrane region of the PTH-1



- receptor. *J Biol Chem* 2001;276:49003-12.
17. Shimizu M, Carter PH, Khatri A, Potts JT Jr, Gardella TJ. Enhanced activity in parathyroid hormone-(1-14) and -(1-11): Novel peptides for probing ligand-receptor interactions. *Endocrinology* 2001;142:3068-74.
  18. Horiuchi N, Holick MF, Potts JT Jr, Rosenblatt M. A parathyroid hormone inhibitor *in vivo*: design and biologic evaluation of a hormone analogue. *Science* 1983;220:1053-5.
  19. Nutt RF, Caulfield MP, Levy JJ, Gibbons SW, Rosenblatt M, McKee RL. Removal of partial agonism from parathyroid hormone (PTH)-related protein-(7-34)NH<sub>2</sub> by substitution of PTH amino acids at positions 10 and 11. *Endocrinology* 1990;127:491-3.
  20. Takasu H, Guo J, Bringhurst FR. Dual signaling and ligand selectivity of human PTH/PTHrP receptor. *J Bone Miner Res* 1999;14:11-20.
  21. Davis DG, Bax A. Assignment of complex 1H NMR spectra via two-dimensional homonuclear Hartmann-Hahn spectroscopy. *J Am Chem Soc* 1985;107:2820-1.
  22. Jeener J, Meier BH, Bachman P, Ernst RR. Investigation of exchange processes by two-dimensional NMR spectroscopy. *J Chem Phys* 1979;71:4546-53.
  23. Rance M, Sorensen OW, Bodenhausen G, Wagner G, Ernst RR, Wuthrich K. Improved spectral resolution in COSY <sup>1</sup>H-NMR spectra of proteins via double quantum filtering. *Biochem Biophys Res Commun* 1983;117:479-85.
  24. Marion D, Wuthrich K. Application of phase sensitive two-dimensional correlated spectroscopy (COSY) for measurements of <sup>1</sup>H-<sup>1</sup>H spin-spin coupling constants in proteins. *Biochem Biophys Res Commun* 1983;113:967-74.
  25. Driscoll PC, Gronenborn AM, Beress L, Clore GM. Determination of the three-dimensional solution structure of the antihypertensive and antiviral protein BDS-1 from the sea anemone *Anemonia sulcata*: A study using nuclear magnetic resonance and hybrid distance geometry-dynamical simulated annealing. *Biochemistry* 1989;28:2188-98.
  26. Nilges M, Clore GM, Gronenborn AM. Determination of three-dimensional structures of proteins from interproton distance data by hybrid distance geometry-dynamical simulated annealing calculations. *FEBS Lett* 1988;229:317-24.
  27. Nilges M, Clore GM, Gronenborn AM. Determination of three-dimensional structures of proteins from interproton distance data by dynamical simulated annealing from a random array of atoms. Circumventing problems associated with folding. *FEBS Lett* 1988;239:129-36.
  28. Nilges M, Gronenborn AM, Brunger AT, Clore GM. Determination of three-dimensional structures of proteins by simulated annealing with interproton distance restraints. Application to crambin, potato carboxypeptidase inhibitor and barley serine proteinase inhibitor 2. *Protein Eng* 1988;2:27-38.
  29. Brunger AT, Adams PD, Clore GM, DeLano WL, Gros P, Grosse-Kunstleve RW, et al. Crystallography & NMR System: A New Software Suite for Macromolecular Structure Determination. *Acta Cryst* 1998;D54:905-21.
  30. Wuthrich K. *NMR of Proteins and Nucleic Acids*. New York: Wiley; 1986.